

Raman scattering in carbon nanotubes

C. Thomsen

Technische Universität Berlin, Hardenbergstrasse 36, 10623 Berlin, Germany

ABSTRACT

For the correct interpretation of Raman spectra it is important to realize that the scattering process in carbon nanotubes is doubly resonant, a feature which – although known from semiconductors – is greatly enhanced by the peculiar bandstructure of graphene near the K -point. We discuss the double-resonant process and, as examples of its importance, show how the relative defect concentration in a set of boron-doped multiwalled tubes can be measured and how the determination of the diameter through the radial breathing mode (RBM) is affected by double resonance.

Keywords: Raman scattering, carbon nanotubes, radial breathing mode, defect concentration

1. INTRODUCTION

Raman scattering has become an important tool in the investigation of carbon nanotubes. Its *in situ* capability and its non-destructive character make it ideal to study the diameter, the metallic or semiconducting property and the concentration of defects. In addition, one can study the orientation of individual nanotubes which is of technological importance. Single-molecule spectroscopy is possible because of the extremely large absolute Raman scattering cross section, which recently was measured and calculated.¹ At 2.05 eV, *e.g.*, the Raman cross section of a (10,10) nanotube RBM is four orders of magnitude larger than the first-order phonon of Si at 520 cm^{-1} .

2. DOUBLE-RESONANT RAMAN SCATTERING IN GRAPHITE

Key to understanding the Raman spectra in carbon nanotubes is the strong excitation-energy dependent Raman shift of the so-called D -mode, which exists in nanotubes and graphite.² Such a shift is not expected in non-resonant or singly-resonant Raman spectroscopy, where due to momentum conservation and due to the small momentum of incoming and scattered light the phonons observed in the Raman spectra originate from the center of the Brillouin zone (Γ -point). From this point of view, changing the incident photon energy changes the electronic resonance condition for the incident or scattered light, the energy of the emitted (or, in anti-Stokes scattering, absorbed) phonon, however, remains unchanged. Only for scattering off excitations with a non-zero dispersion at the Γ -point, such as acoustic phonons, the energy of the excitation studied in Raman shifts with laser energy. Single resonances have been extensively used to study electronic properties of semiconductors in the past, see, *e.g.*, Cardona.³

A Raman process is double resonant, if two real transitions occur, a condition which is rarely fulfilled for Γ -point phonons but can be met more easily if large phonon wave vectors are allowed. A simple schematic of the double-resonant Raman process is shown in Fig. 1 for parabolic bands, as they occur for instance for metallic nanotubes near the K -point. For a given incident photon energy, there is an incoming-photon resonance, as long as the photon energy is larger than the gap energy. In a second step, the electron is scattered resonantly across the band minimum by a phonon. Then, a defect is invoked to scatter the electron elastically back near (in k -space) to where it was absorbed, and finally the electron recombines with the hole in a vertical, $k \approx 0$ transition. (The last two steps are not shown in Fig. 1.) It is to be noted that the defect at this point is merely needed to conserve momentum in the recombination process; the defect is taken to scatter without changing the symmetry of the excitation or its energy, which is the simplest possible assumption about this process. As we will see later, the signal in the Raman spectra are indeed proportional in amplitude to the number of defects induced either by doping or by irradiation, confirming this picture. Secondly, we note that different time-ordered

contact information: E-mail: thomsen@physik.tu-berlin.de

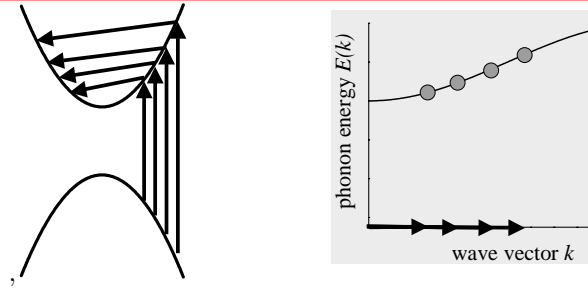


Figure 1. 1D-schematic double-resonant Raman process as it occurs, for example, in carbon nanotubes. The incident photon is absorbed in a vertical transition, causing an incoming resonance for energies larger than the band gap. The electron is then scattered resonantly by a phonon across the band minimum; larger incident photon energies correspond to larger phonon scattering vectors (*left*). If the phonon is dispersive, different phonon energies are seen in the Raman spectra (*right*).

processes also occur, *i.e.*, the defect first scatters inelastically, and then the phonon scatters the electron back to where it was absorbed, or other time orders. A full calculation of the scattering signal involves all possible time orders of the processes absorption, scattering by the phonon, scattering by the defect, and recombination.^{4,5}

Given that the *D*-mode as well as the HEM are defect induced by the double-resonance process, they should provide a means of determining – at least relatively – the defect concentration in a set of samples. Such experiments were performed in boron-doped multiwalled samples⁶ and, in single-walled nanotubes.⁷ We show here the results of Maultzsch *et al.*⁶ for 0.5, 1.0, and 4.0 % boron-dopant concentration in the rods used for arc discharge in preparation. The physically meaningful way of normalizing the spectra is with respect to the area of the second-order mode at $\approx 2600 \text{ cm}^{-1}$. This peak is related to emitting two phonons with equal and opposite momentum and is – to first approximation – independent of the number of defects for a not too high concentration of defects in a sample. Such analysis yields the slopes as function of boron concentration, which – once calibrated – can readily be used to determine the number of defects in a particular sample as shown in Fig. 2. The slope may be expressed as⁶

$$\begin{aligned} I^{D/D^*} &= 1.3 + 1.40 x (\% \text{ boron conc.})^{-1} \\ I^{HEM/D^*} &= 2.1 + 0.47 x (\% \text{ boron conc.})^{-1} \end{aligned} \quad (1)$$

and allow an *in situ* determination of the defect concentration in a particular nanotube sample. Qualitatively similar slopes were found by Skakalova *et al.* for single-walled nanotubes with defects created by γ -radiation.⁷

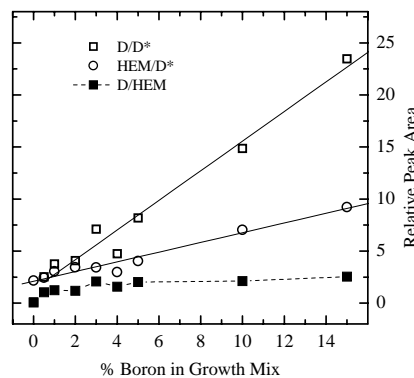


Figure 2. Relative peak area of the *D*-mode and the HEM normalized to the second-order *D** peak in carbon nanotubes. The slopes are given in the text, Eqn. (1). From Maultzsch *et al.*⁶

3. DOUBLE-RESONANT SCATTERING IN CARBON NANOTUBES

The double-resonant scattering process has become a well-established process describing a number of features of the Raman spectra of sp^2 bonded carbon compounds such as graphite or carbon nanotubes.^{2, 4, 5} For the D -mode in graphite, bundles of single-walled nanotubes and so-called bucky pearls this shift amounts to $50\text{-}60\text{ cm}^{-1}/\text{eV}$ excitation energy, and is much larger than when observed, *e.g.*, in GaAs quantum wells⁸ or Ge.⁹ The high-energy mode (HEM) at 1590 cm^{-1} , sometimes referred to as G -mode, also displays excitation-energy dependent shifts;⁴ they are smaller and sometimes missed in the literature when not evaluated over a large enough energy range.¹⁰ In Fig. 3 we present the Raman spectra of bucky pearls, which clearly show how the 2nd and 3rd largest peak in the HEM shift to lower energies when excited with increasing photon energies. In contrast to this behavior is that of the G -mode in graphite, which is constant in energy¹¹ for excitations ranging from 1 to 4 eV and thus singly resonant.

In an alternative attempt to explain the excitation-energy dependence in nanotubes some authors have been focussing on the strength of the van-Hove singularity in the electronic transition of the nanotube.^{5, 12} These authors take the view that a nanotube contributes to the Raman signal significantly only near the maximum in the density of states. Varying the excitation energy then selects a different nanotube with a different phonon energy. In this way, an ensemble of tubes with a typical diameter distribution may yield apparently varying Γ -point phonon frequencies in a sample with a distribution of tube diameters. The two different views are summarized in Fig. 4. In the double-resonant picture the excitation-energy dependence reflects the phonon dispersion in an individual nanotube, while in the single-resonant view it resembles a diameter and chirality distribution. Because of the important consequences for the interpretation of the Raman spectra a distinction between these two processes is vital and, clearly, an experiment on an individual, isolated nanotube can distinguish the two types of resonances.

We performed such single-tube experiments on HiPco produced nanotubes, which were solution cast onto marked substrates. The density of tubes was $\sim 0.5\text{ tubes}/\mu\text{m}^2$. We used various laser lines of an Ar/Kr laser and a number of frequencies of a dye laser for excitation. The spectra were dispersed by a Dilor XY triple spectrometer and detected by a CCD detector.

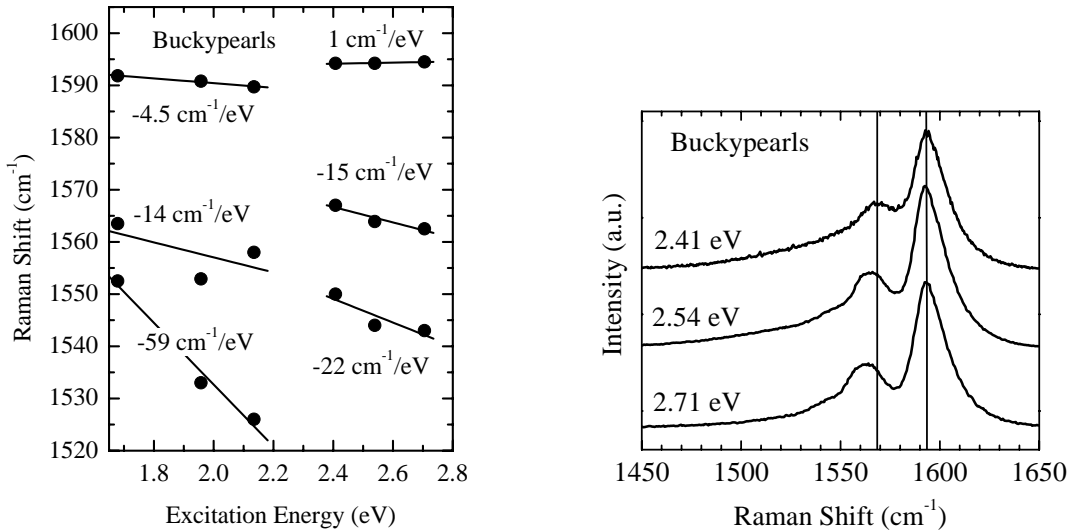


Figure 3. *left:* Peak frequencies in the range of 1.7 to 2.7 eV excitation energy. All peaks have an excitation-energy dependence; it is due to the double-resonance process. The jump in absolute phonon energies and slopes at 2.3 eV is due to a higher electronic band involved in the double resonance as explained by Maultzsch *et al.*⁴ *right:* Raman spectra of bucky pearls excited at three different laser energies. Clearly seen is the downshift of the second largest peak for increasing photon energy.

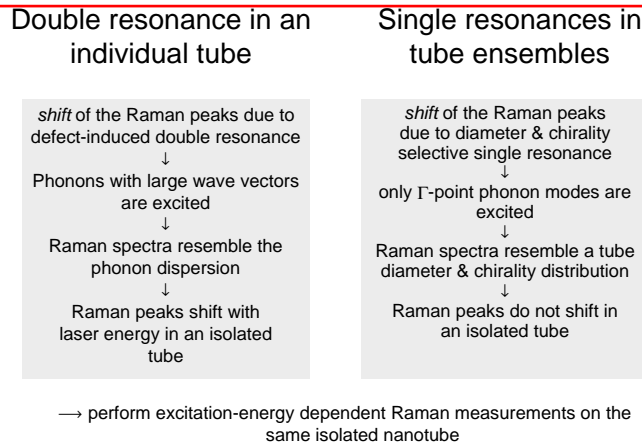


Figure 4. Flow chart for distinguishing double (*left*) from single (*right*) resonances. Excitation-energy dependent Raman spectra on individual nanotubes can distinguish between these two possible processes.

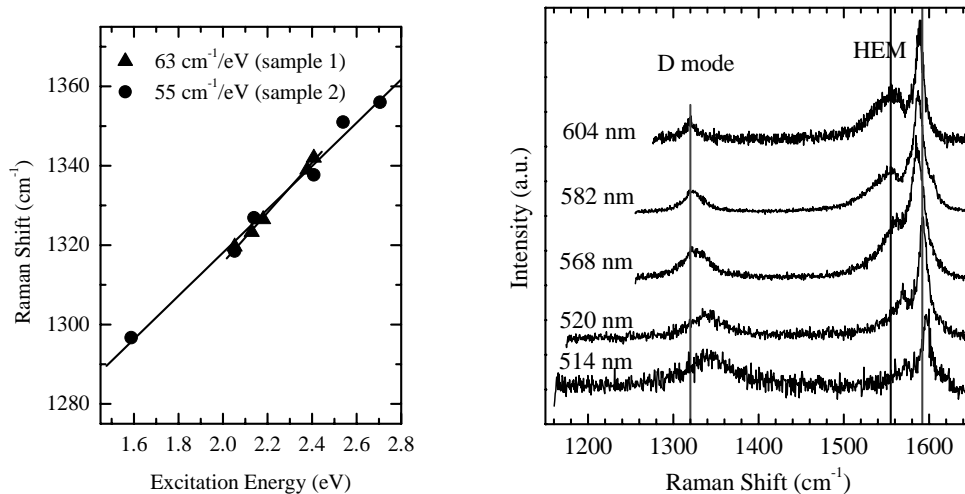


Figure 5. *left*: Frequency-dependence of the *D*-mode for two different isolated nanotubes; *right*: Raman spectra on an isolated or a nearly isolated nanotube. From Maultzsch *et al.*¹⁴

The Raman spectra obtained are shown in Fig. 5. On the right we show the high-energy region and make the following observations: 1) the *D*-mode shifts continuously to higher energies with 55-65 cm⁻¹/eV [Fig. 5 (*left*)]. 2) The high-energy mode frequency varies as well, the highest peak first decreases, then increases; the second largest peak increases monotonically in frequency. 3) The lineshape of the high-energy mode changes continuously from a more metallic to a more semiconducting appearance. In the low-energy region (not shown) we find a strong RBM mode at 250 cm⁻¹, which slightly shifts when increasing the photon energy and then becomes weaker, disappearing for the highest photon energies measured.

All observations fall naturally into the double-resonance interpretation and are incompatible with the single resonance view. 1) The *D*-mode in the individual tube or thin bundle shifts at the same rate as in bulk samples; 2) The high-energy mode resembles the dispersion of a metallic tube. In such tubes the LO-like mode has been shown¹³ to soften to about 1550 cm⁻¹. 3) The lineshape changes continuously from metallic-looking to semiconducting-looking, and is due to scattering near the band minimum (~ 2.0 eV; metallic looking) and far away from it (~ 2.4 eV; semiconducting looking), see Fig. 6, *left*, for a schematic. Detailed calculations of the lineshape-dependence on excitation energy are under way.¹⁵

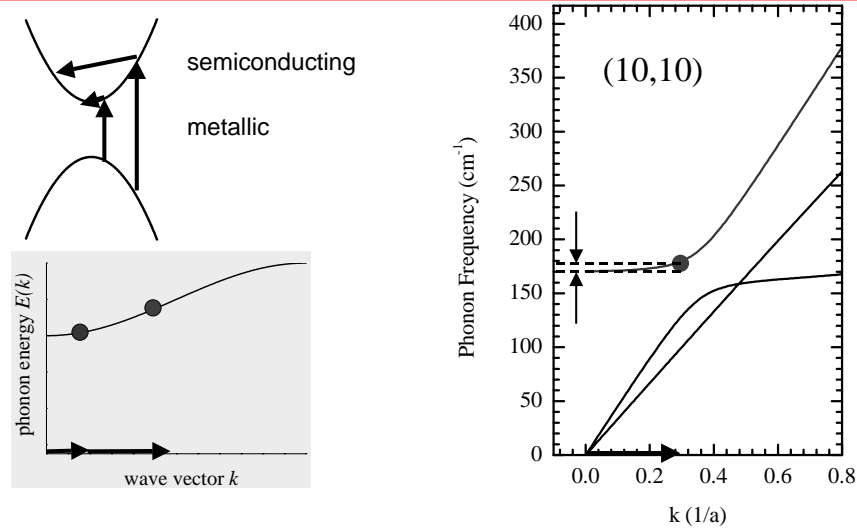


Figure 6. *left:* Schematic view of how metallic-like (optical transition near the band minimum) and semiconducting-like Raman peaks occur within one nanotube. *right:* Expanded view of the radial breathing mode near the Γ -point of the Brillouin zone of a (10,10) tube. Indicated is the shift of the peak frequency observed in double-resonant Raman scattering compared to the true Γ -point frequency.

4. DOUBLE RESONANCE AND THE RBM MODE

We discuss now another important implication for the interpretation of the Raman spectra of carbon nanotubes. The RBM is frequently used to determine the diameter of a nanotube to an extraordinarily high precision.^{12, 16, 17} While the inverse-diameter dependence of the RBM frequency is generally accepted (for deviations at small diameters, see Kürti *et al.*¹⁸) the underlying assumption is that the RBM as observed in the Raman spectra is a Γ -point mode. If double resonant, however, this is no longer true and serious shifts occur in the RBM frequency, making the chiral-index analysis unreliable. In Fig. 6 we show the low-energy, low- k region of the phonon dispersion relations of a (10,10) nanotube.^{19, 20} For a typical double-resonant phonon wave vector (~ 0.3 $1/a$) the dispersion-induced shift in a (10,10) tube corresponds to ~ 10 cm^{-1} . Obviously, the precise shift depends on the phonon dispersion and on the incident photon energy, but it should be clear that the simple RBM frequency-diameter correspondence does not hold very well in the double-resonance picture.

5. CONCLUSION

In summary, excitation-energy dependent Raman experiments on isolated tubes have established double-resonant Raman scattering as the dominant mechanism for carbon nanotubes over diameter and chirality-selective scattering. We showed how the concentration of defects can be determined from comparing first and second-order peaks and we discussed important consequences for the interpretation of the RBM frequency-diameter relation, and for the metallic and semiconducting appearance of the high-energy mode.

I thank J. Maultzsch and S. Reich for valuable discussions on the topic and J. Maultzsch for a critical reading of the manuscript. U. Schlecht provided the samples for the measurements on isolated nanotubes.

REFERENCES

1. M. Machón, S. Reich, J. Maultzsch, P. Ordejón, and C. Thomsen, submitted to Phys. Rev. Lett.
2. C. Thomsen and S. Reich, Phys. Rev. Lett. **85**, 5214 (2000)
3. M. Cardona, in: Light Scattering in Solids II, Topics in Applied Physics, Vol. 50, ed. M. Cardona and G. Güntherodt (Springer, New York, Heidelberg, 1989).
4. J. Maultzsch, S. Reich, and C. Thomsen, Phys. Rev. B **65**, 233402 (2002)

5. J. Kürti, V. Zólyomi, A. Grüneis, and H. Kuzmany, *Phys. Rev. B* **65**, 165433 (2002)
6. J. Maultzsch, S. Reich, C. Thomsen, S. Webster, R. Czerw, D.L. Carroll, S.M.C. Vieira, P.R. Birkett, and C.A. Rego, *Appl. Phys. Lett.* **81**, (17) 2647-49 (2002)
7. V. Skakalova *et al.*, in: *Electronic Properties of Novel Materials – Progress in Molecular Nanostructures*, eds. H. Kuzmany, J. Fink, M. Mehring, and S. Roth, IWEPNM Kirchberg (2003), in print.
8. V.F. Sapega, M. Cardona, K. Ploog, E.L. Irchenko, and D.N. Mirlin, *Phys. Rev. B* **45**, 4320 (1990)
9. D.J. Mowbray, H. Fuchs, D.W. Niles, M. Cardona, C. Thomsen, B. Friedl, 20th International Conference on the Physics of Semiconductors, eds. E.M. Anastassakis and J.D. Joannopoulos, Thessaloniki, Greece, (World Scientific, Singapore, 1990), p. 2017
10. A. Jorio, M. A. Pimenta, A. G. Souza Filho, Ge. G. Samsonidze, A. K. Swan, M. S. nl, B. B. Goldberg, R. Saito, G. Dresselhaus, and M. S. Dresselhaus *Phys. Rev. Lett.* **90**, 107403 (2003)
11. I. Pócsik, M. Hundhausen, M. Koos, O. Berkese, and L. Ley, in *Proceedings of the XVI International Conference on Raman Spectroscopy*, ed. A.H. Heyns (Wiley-VCH, Berlin, 1998) p. 64
12. A. Jorio, R. Saito, J.H. Hafner, C.M. Lieber, M. Hunter, T. McClure, G. Dresselhaus, and M. Dresselhaus, *Phys. Rev. Lett.* **86**, 118 (2001)
13. O. Dubay, G. Kresse, and H. Kuzmany, *Phys. Rev. Lett.* **88**, 235506 (2002)
14. J. Maultzsch, S. Reich, U. Schlecht, and C. Thomsen, *Phys. Rev. Lett.* (2003), in print.
15. J. Maultzsch *et al.*, to be published
16. R. Pfeiffer, C. Kramberger, C. Schaman, A. Sen, M. Holzweber, H. Kuzmany, H. Kataura, Y. Achiba, in: *Electronic Properties of Novel Materials – Progress in Molecular Nanostructures*, eds. H. Kuzmany, J. Fink, M. Mehring, and S. Roth, IWEPNM Kirchberg (2003), in print.
17. M. S. Strano, S. K. Doorn, E. H. Haroz, C. Kittrell, R. H. Hauge, and R. E. Smalley, *Nano Lett.* (2003), to be published, DOI: 10.1021/n1034196n.
18. J. Kürti and V. Zólyomi, in: *Electronic Properties of Novel Materials – Progress in Molecular Nanostructures*, eds. H. Kuzmany, J. Fink, M. Mehring, and S. Roth, IWEPNM Kirchberg (2003), in print.
19. M. Damnjanović, T. Vuković and I. Milosević, *J. Phys. A* **33**, 6561 (2000)
20. E. Dobardžić, I. Milošević, B. Nikolić, T. Vuković, and M. Damnjanović *Phys. Rev. B* **68**, 045408 (2003)